SACLANT UNDERSEA RESEARCH CENTRE REPORT
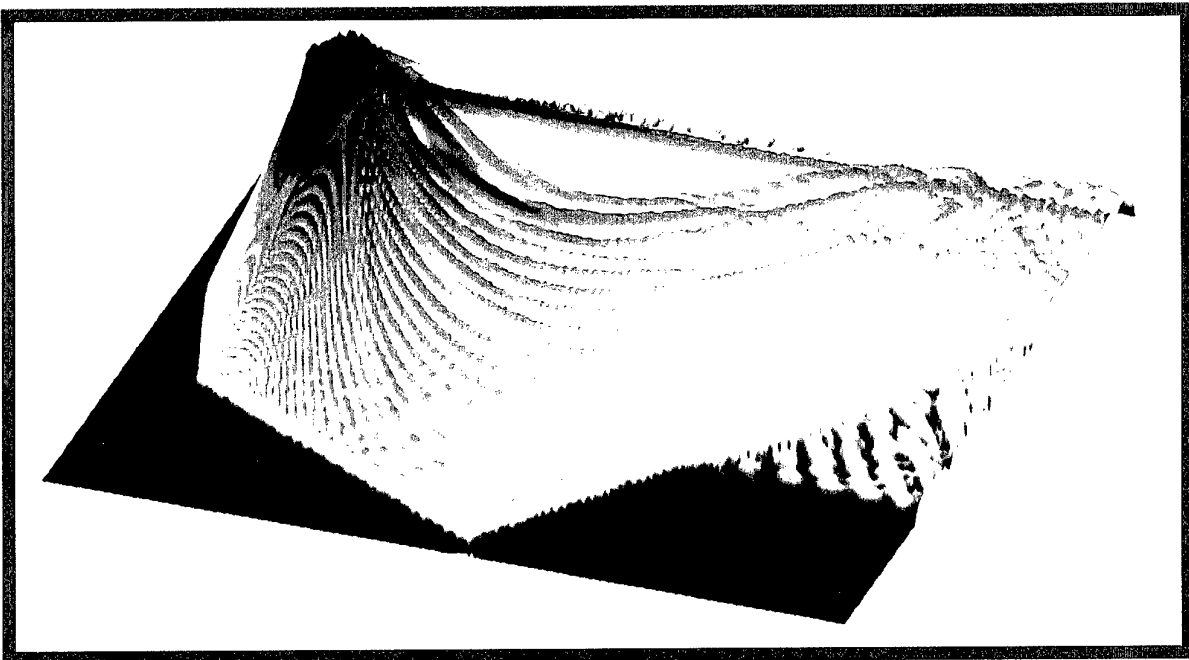
DISTRIBUTION STATEMENT A
Approved for Public Release
Distribution Unlimited

20010515 046

NORTH ATLANTIC TREATY ORGANIZATION   ORGANISATION DU TRAITE DE L'ATLANTIQUE NORD

SWAC 4: Broadband data analysis using sub-band processing - part II

G. Haralabus, E. Capriulo

The content of this document pertains
to work performed under Project 04-A of
the SACLANTCEN Programme of Work.
The document has been approved for
release by The Director, SACLANTCEN.

Jan L. Spoelstra
Director

intentionally blank page

SWAC 4: Broadband data analysis using sub-band processing - part II

G. Haralabus, E. Capriulo

Executive Summary:

Reverberation caused by anomalies and abrupt bathymetric changes degrades the detection performance of sonar systems, especially when the target is located near the clutter area. In a reverberation limited environment, the utilization of broadband signals can improve detection and localization either by reduction of the resolution cells insonified by the sonar or by frequency optimization, according to which the detection algorithm is applied selectively to the spectrum regime(s) which maximize(s) the signal-to-reverberation ratio. This report examines the frequency variability of reverberation induced by a 2300-3500 Hz LFM signal.

The 1200-Hz bandwidth is divided into ten equal sub-bands, each of which is processed individually through a matched filter. The results are compared to reveal the frequency dependence of reverberation induced by a 200 m seafloor mount. The present report is the sequel to SR-320. The analyzed data do not contain submarine echoes.

intentionally blank page

SWAC 4: Broadband data analysis
using sub-band processing - part II

G. Haralabus, E. Capriulo

Abstract:

The frequency dependence of reverberation is examined using the processing method as for the frequency analysis of target detection during the same experiment.

In this experiment, reverberation is induced by abrupt changes in the bottom bathymetry (a 200 m sea mount). For the analysis of the received signal a sub-band matched filter scheme is devised, according to which, a replica of the transmitted pulse (2300-3500 Hz LFM signal) is segmented into ten 120 Hz sub-bands, each of which is processed independently through a matched filter detector. Following the necessary corrections for array gain and calibration, transmitted power spectrum and propagation loss, the matched filtered data are compared to reveal the frequency dependence of reverberation. Due to insufficient *in situ* measurements, the propagation loss estimate is based on model calculations - a challenging task for the range dependent seafloor at the experimental site.

After examining a large number of pings it is concluded that the reverberation energy calculated at the correlator output is comparable for all ten sub-bands. This leads to the conclusion that for the particular environment and experimental geometry, the frequency spectrum is not sufficiently wide to allow significant frequency variability which may indicate an optimum operational frequency.

Contents

1

Introduction

The utilization of broadband signals is widespread in the underwater community for a number of reasons the most important of which is reverberation suppression. Reverberation, caused by anomalies and abrupt bathymetric changes significantly degrades the detection performance of sonar systems, especially when the target is located near the clutter area. Detection performance may be improved by identifying and exploiting spectral differences between reverberation and target echoes.

The data were acquired during the SWAC-4 sea trial. The spectral comparison between the target and the reverberation signal is performed separately. The frequency sensitivity of the target detection can be found in [1]. This report examines the frequency diversity of monostatic (active) reflection of a 200 m seamount, using the same processing method as in [1]. During the experiment, a 1200 Hz LFM centered around 3 kHz was transmitted. In post-processing, a replica of this signal is divided into ten sub-bands and the matched filter (MF) algorithm is applied to each one. Comparison of the MF outputs reveals the frequency dependence of reverberation.

2

Experimental configuration and data acquisition

The data were acquired during run 18 of the SWAC 4 sea trial which took place in the Ionian sea in 1996. The run commenced at 05:51 ending at 08:06 Zulu time. A total of 180 pings were transmitted in a closing-opening type of run. The average speed of the ship was 5.2 kn. Figure 1 shows a bathymetric map of the area, the course of the *R. V. Alliance* and the reverberation area. Figure 2 shows the bathymetry and the sound velocity profiles (SVP) used between the source and the receiver. The first profile (shallow area) was the only one measured from the source ship; the others are replicas of the first one with the negative gradient extended to the corresponding bottom depth.

The transmitted signal is a 12 s, uniform LFM with frequencies 2300 Hz to 3500 Hz. The receiving device is a 64-element, mid frequency, horizontal array. 21 beams are formed. The sampling frequency (after undersampling) is 4000 Hz. The length of the acquisition window is 55 s (including the 12 s transmission) plus a 5 s waiting period which results in a one ping per minute repetition rate.

Figure 3 shows the 2-D propagation loss contour plots for the low and the high end of the spectrum using the parabolic equation model PAREQ [3]. The modeling issues are discussed in detail in the following chapters. From this figure it can be observed that sound propagation in the water column follows a similar pattern for the two frequencies. In both cases there is a distinct sound channel axis at approximately 68 m (source depth). The abrupt bathymetric changes guide the sound in and out of a 200 m trench. The reverberation field is produced by the reflection of the transmitted pulse at the upslope part of the trench.
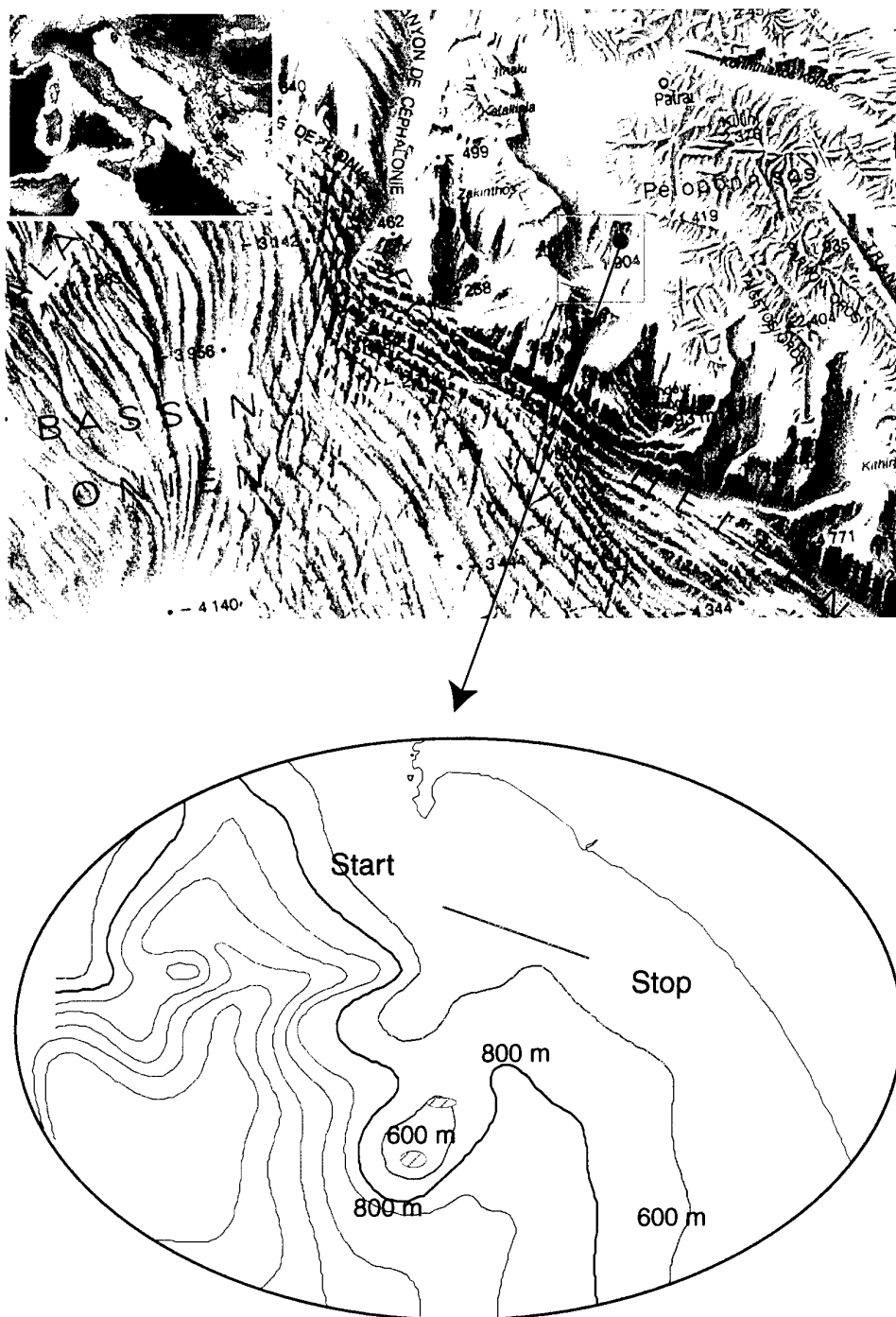
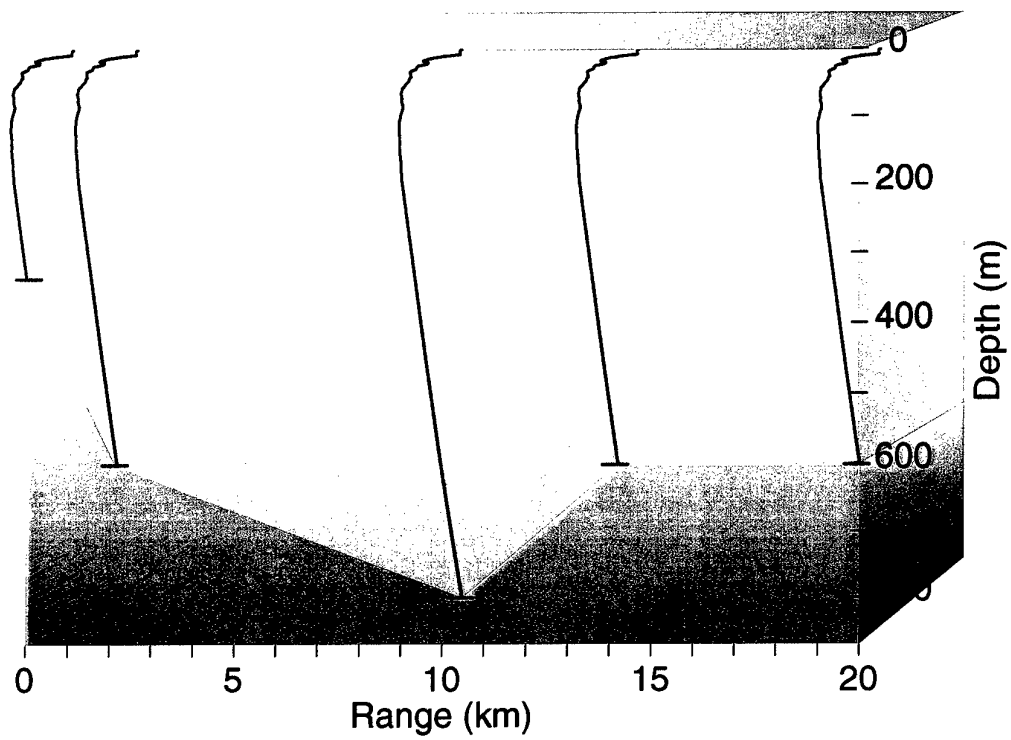**Figure 1** *Experimental site of the SWAC 4 sea trial and run geometry with bathymetry measurements.*

Figure 2 *A design of the seafloor bathymetry and the sound velocity profiles in the water column.*
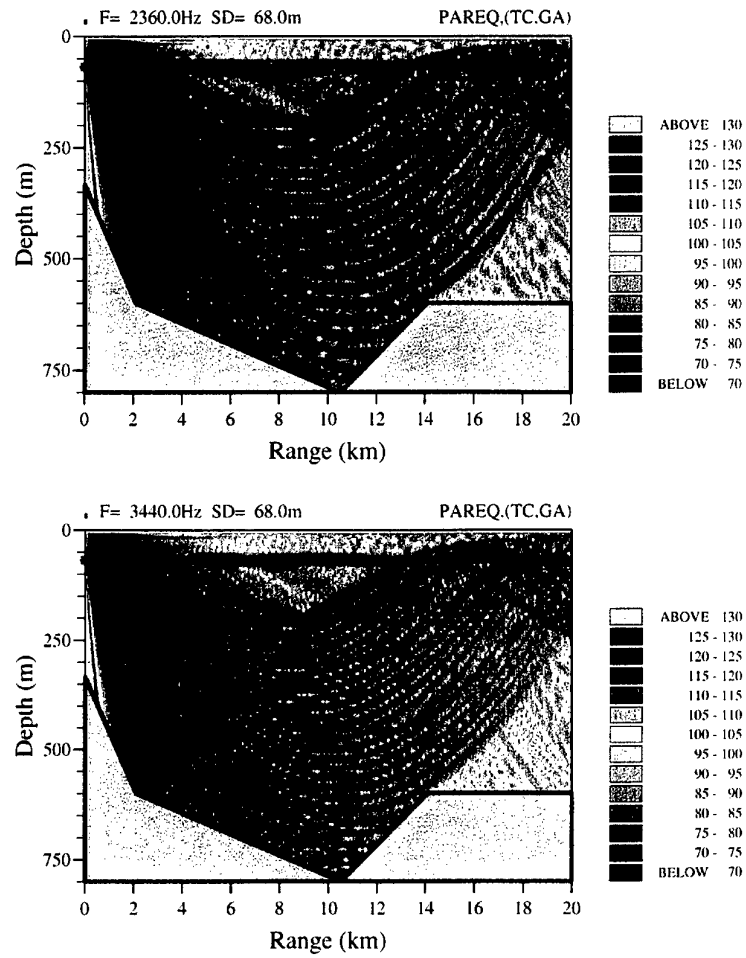
Figure 3 *Low (2360 Hz) and high (3440 Hz) frequency propagation loss contour plots. Distinct sound channel axis at 68 m.*

3

Frequency variability of reverberation based on sub-band processing

The transmitted LFM spectrum ranges from 2300 to 3200 Hz. It is divided into ten sub-bands and ten LFM replicas of 120 Hz bandwidth are created. The replicas are correlated with the full band of the received reverberation signal using the MF processor.

Figures 4, 5 show the reverberation signal for the low (2300-2420 Hz) and the high (3380-3500 Hz) sub-band in a 13 ping sequence (from ping 70 to ping 130) with a 5 ping step increment. Ping 70 corresponds approximately to the middle of the run, when the source is closing with the clutter area (see Fig. 1). Ping 130 corresponds to the end of the run as the distance between the source and the clutter increases (opening part). This closing-opening pattern is clearly observed in Fig. 4 and 5. Each ping is represented by a set of 11 beams (beam 5 to beam 15), marked in a counter-clockwise fashion counting from the endfire opposite to the direction of the ship. This explains why for the low ping numbers (closing part of the run), the reverberation is captured by the high beams (10,11,12) while for the high ping numbers (opening part of the run), the reverberation is received by the lower beams (8,9).

The characteristics of both sub-bands are similar although the background noise level is higher in low than in high frequencies. The first 6 pings insonify a more extended reverberation area than the last 5 pings due to the different aspect angle. To obtain a comparable reverberation estimate, calculations were limited to the initial reverberation zone which is common for all cases. The average reverberation power is calculated over a 2 km range around the highest reverberation zone for each ping, based on the best five beams for each ping (the results are similar for the two-beam average). Figure 6 shows the average reverberation values in dB (adjusted for array gain and calibration) as a function of frequency (sub-band) for 13 pings. The x-axis has 10 points, each of which corresponds to a sub-band, e.g 1 corresponds to 2300-2420 Hz, 2 to 2420-2540, ..., 10 to 3380-3500 Hz. The 13 pings (70 to 130, step 5) are colour differentiated. The first two pings, i.e. 70 and 75, have significantly lower values than the rest as they correspond to that part of the run in which reverberation is building up towards its maximum values. They are maintained in this analysis to indicate the power jump of the returned signal as the clutter area is gradually insonified. The last two low value pings, 125 and

130, correspond to the part of the run where reverberation diminishes. The pings with the highest reverberation values correspond to the minimum distance from the reverberation area varying within a 3 dB zone. In terms of frequency variability all pings have their maxima in the low-mid frequency regime or in terms of sub-bands at 2660-2780 Hz. This observation alone does not lead to any conclusion regarding the actual frequency variability, because the mean reverberation values must be corrected for the source level and the propagation loss. The important information conveyed in this initial estimate is that all pings, in spite of the fact that they have different intensity levels, demonstrate similar characteristics as a function of frequency.
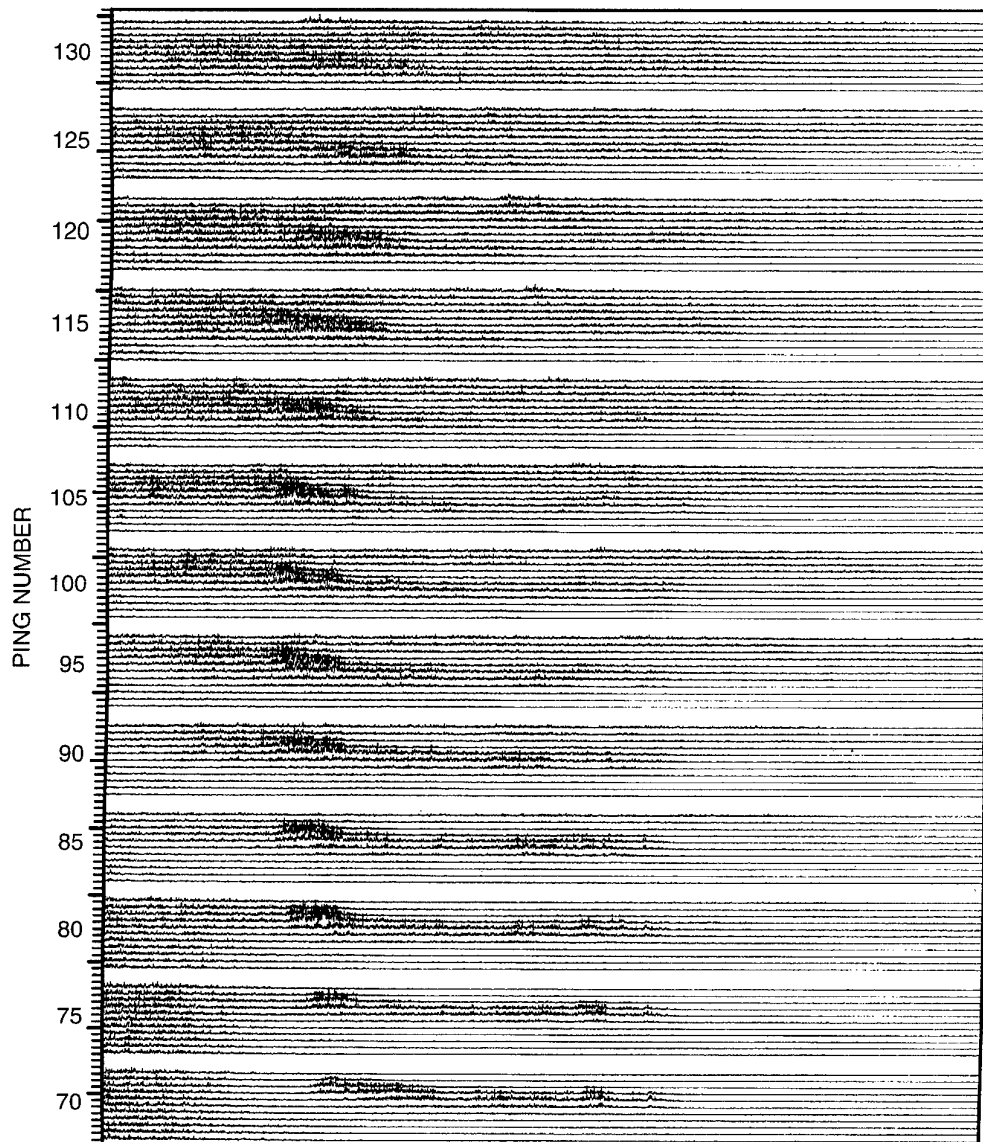
Figure 4 *Matched filter output for the low frequency band (2300-2420 Hz). 13 pings are displayed (70-130 step 5). Each ping includes 11 beams (5-15 step 1 counting unwards).*
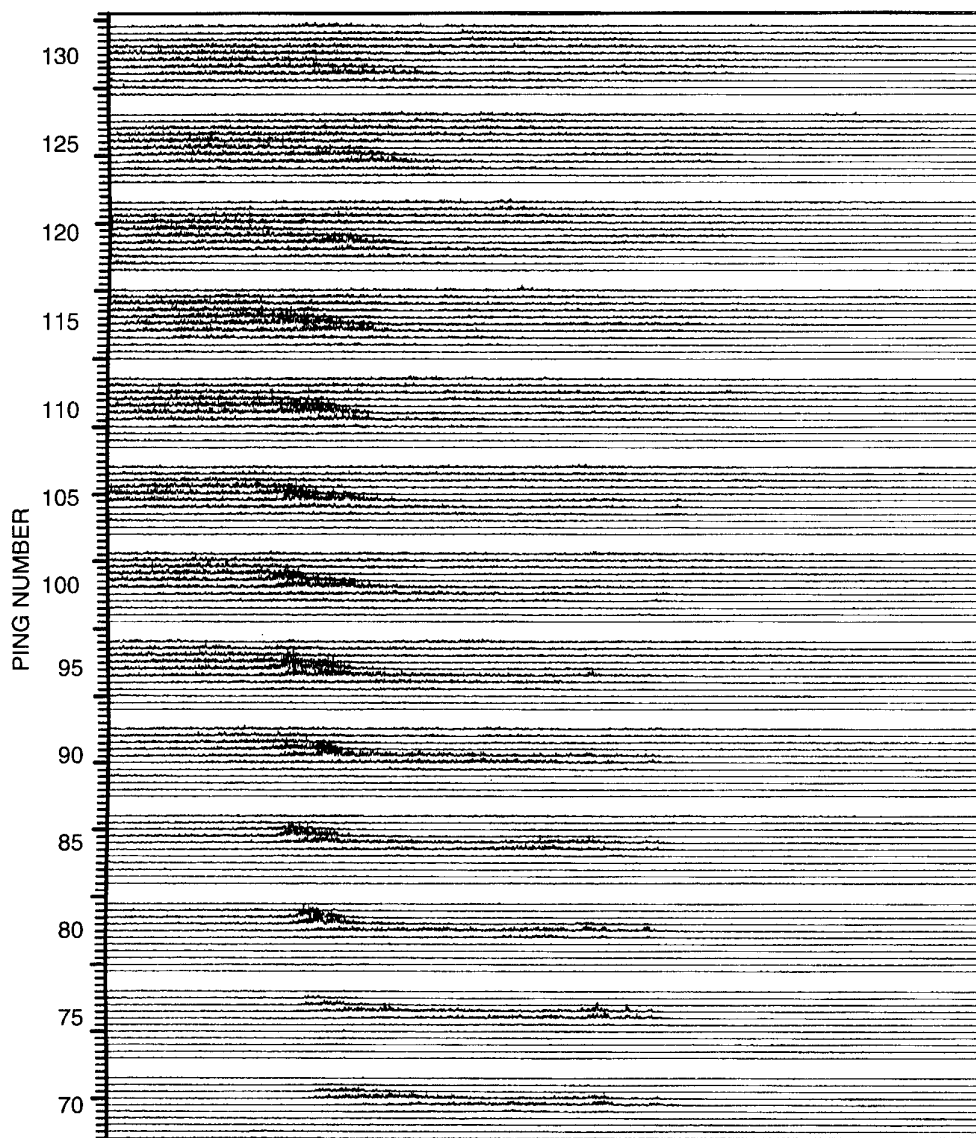
Figure 5 *Matched filter output for the high frequency band (3380-3500 Hz). 13 pings are displayed (70-130 step 5). Each ping includes 11 beams (5-15 step 1 counting unwards).*
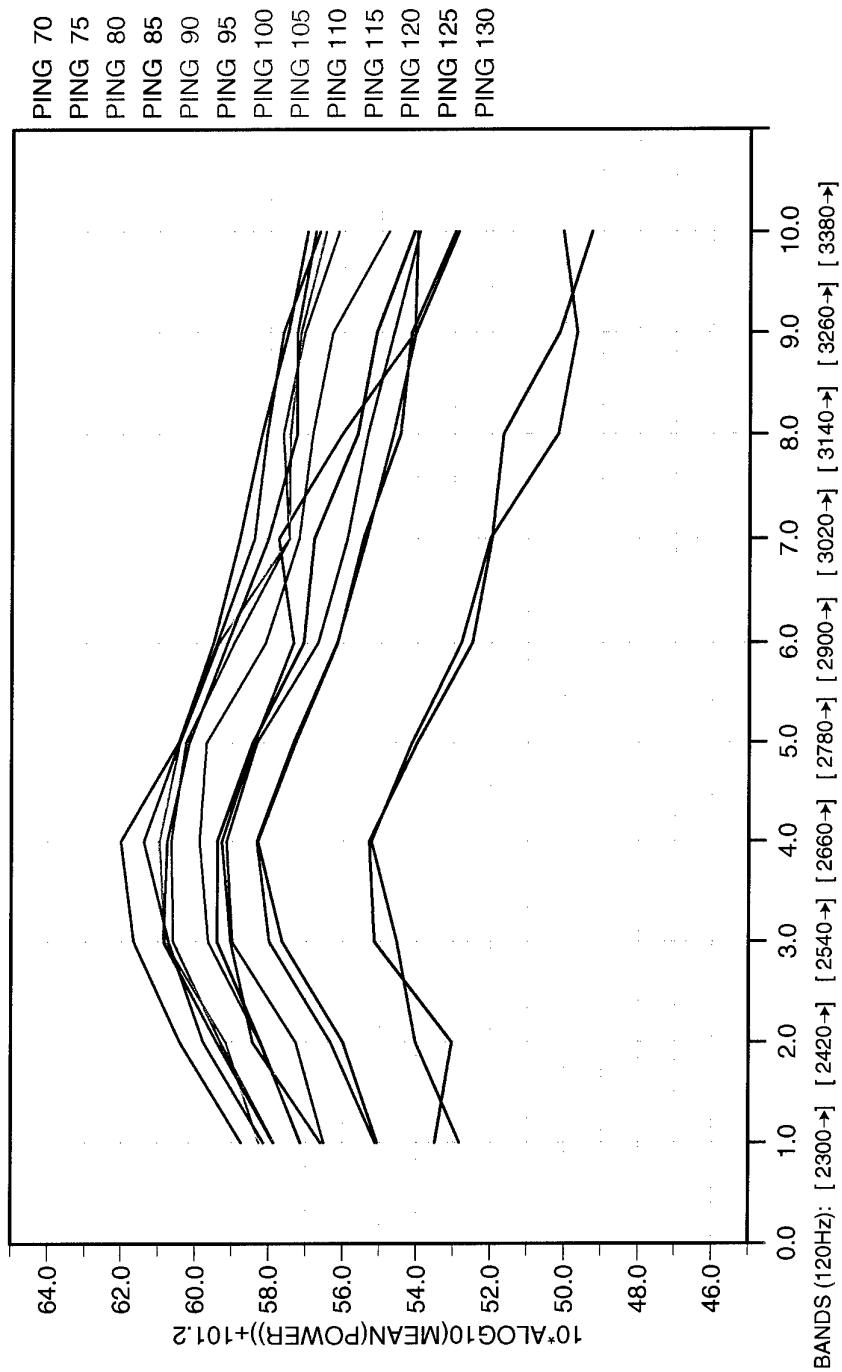
Figure 6 *Average reverberation power versus frequency (sub-bands) for 13 pings which are indicated with different colours.*

4

Reverberation average power correction according to the source spectrum

The amplitude of the source spectrum is reconstructed by interpolating known discrete values (marked with black dots) as shown in Fig. 7. As it is not flat, the power is distributed unequally over the transmitted spectrum so that certain frequencies are enhanced while others are degraded. That explains, to a certain degree, the frequency dependence of reverberation at the MF output (Fig. 6). Overall, the maxima are close to 2800 Hz and the minima at the beginning of the spectrum at 2400 Hz. The differences vary from 2 to 9 dB. This pattern was kept constant during the run to allow comparison of the reverberation levels for all the sub-bands, the power calculations shown in Fig. 6 must be adjusted according to the source spectrum. The result of this correction is presented in Fig. 8. As the compensation for the low frequencies is significantly greater than that for the high frequencies, average reverberation power appears to decrease with frequency. To further improve the reverberation comparison for the ten sub-bands, an additional adjustment should be applied based on the sound propagation loss, as a function of frequency.
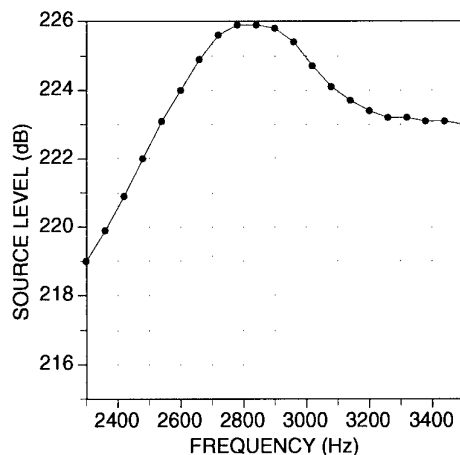

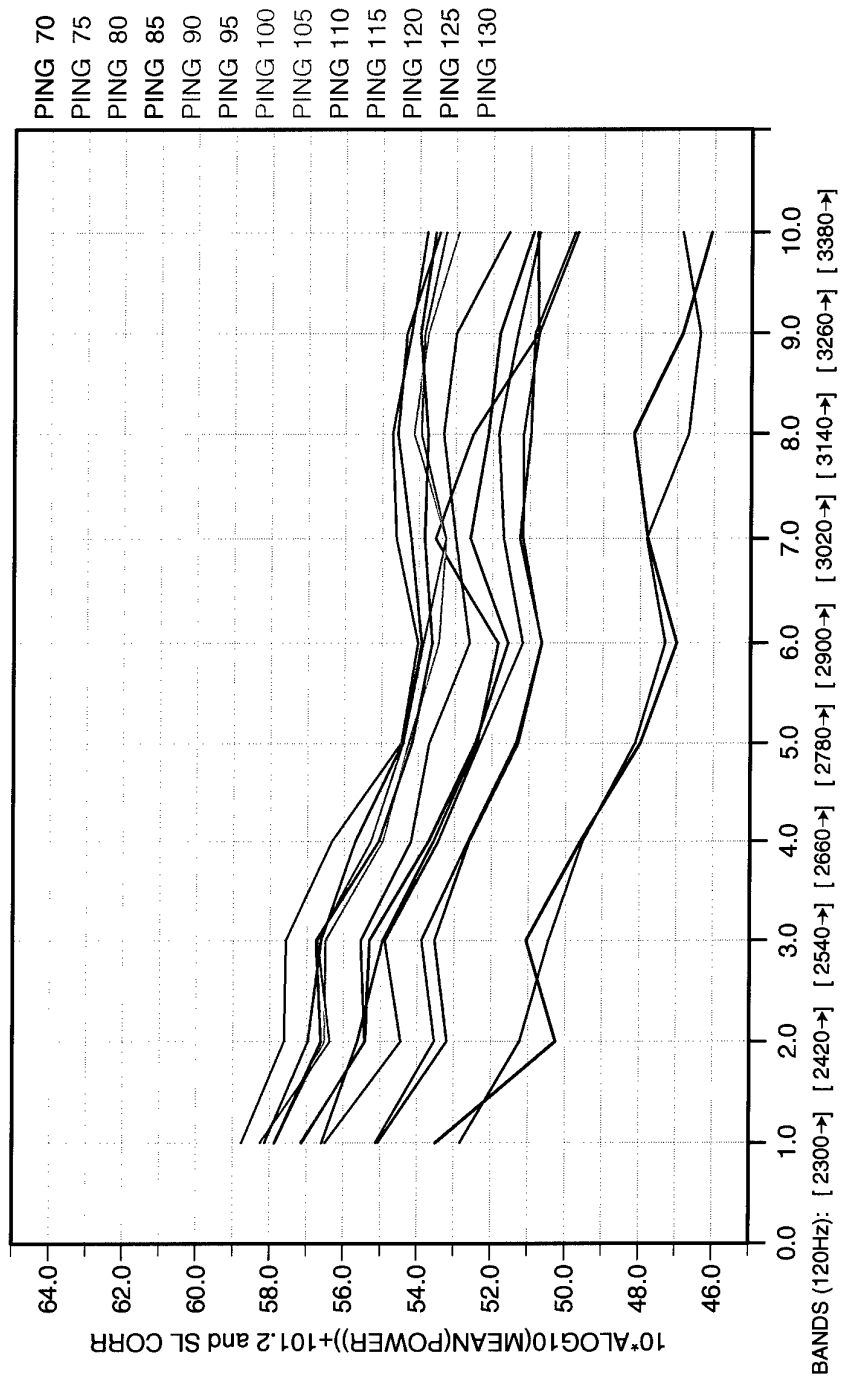**Figure 7** *Source power spectrum used for the correction of the reverberation estimate.*

Figure 8 *Average reverberation power versus frequency after source power correction.*

5

Average reverberation power correction
based on propagation loss estimates

One of the drawbacks of this experiment is the lack of *in situ* sound propagation measurements between the source and the clutter area. This is mainly due to the fact that the original objectives of this experiment did not include the analysis of the reverberation field. To overcome this problem and correct the received echo level with respect to propagation loss as a function of frequency, we rely on acoustic models. It was found that, for the particular environment, the parabolic equation model PAREQ [3] was more appropriate than C-SNAP [4], GRAB [5], and RAM (see Annex A).

The geoacoustic parameters are obtained either from *in situ* measurement or from historical data acquired during previous experiments in the same area. A general propagation loss plot which covers the last 10 km between the source and the clutter area is shown in Fig. 9 (a). The frequency selected is 2360 Hz which is the central frequency of the first sub-band 2300-2420 Hz. Figure 10 (b) is a detail of Fig. 9 (a) focusing on the reverberation area. The black line is the model estimate of the acoustic energy loss due to the medium. The blue, green and red lines represent average values calculated using different methods. The blue line represents a running rectangular window average with 51 samples. Although this technique is incorporated in the acoustic model we decided to compare it with two other methods. The green line represents the Hamming windowing method - a similar type of averaging in the time/range domain. Based on this method, the received time series is convolved with an appropriate Hamming filter. Figure 10 shows a number of Hamming windows, created with different number of samples and the corresponding error functions related to the other two averaging methods. The red line represents averaging in the frequency domain. 13 equally spaced frequencies are selected along the 120 Hz sub-band. The model run is repeated for every frequency and the propagation loss plots are averaged.

The procedure described above is repeated for all the sub-bands and all the ping sets; a total of 169 model runs are executed! The reverberation values are corrected according to twice the average propagation loss estimates to satisfy the two-way propagation conditions. The difference of the two-way propagation loss relative to the minimum value of all sub-bands and all ping cases is presented in Fig. 11. The final results are shown in Fig. 12. The propagation loss correction favors the

high frequencies because, as expected, they underwent a significant energy loss due to the medium. Overall, here is no evidence of a frequency trend, as the small variations which are observed, lie within the statistical variation of the propagation loss estimates.

Although the main concern of this work is the comparison of the reverberation levels corresponding to ten sub-bands, an estimate of the scattering strength is provided as a general verification of the calculations regarding the absolute value of reverberation. As seen previously, the received reverberation level is $RL = 60dB$, the source level $SL = 226dB$ and the two-way propagation loss $TL = 200$ dB. Therefore the unnormalized scattering strength which is $SS_u = SL - TL - RL$ is $SS_u = 34dB$. This figure needs to be normalized by the insonified area on the sea floor $A = \phi r \frac{c\tau}{2}$ where $\phi = 16°$ is the beam angle, $r = 15km$ is the range, $c = 1500m/s$ is the speed of sound, and $\tau = 8.3ms$ is the time corresponding to the inverse of the subband bandwidth. After substitution of the above numbers, the insonified area becomes $A = 26075.28m^2$ or $10log_{10}(A) = 44.1dB$. This means that the normalized scattering strength is $SS = SS_u - 10log_{10}(A) = -10.1\ dB$, which is an acceptable level for hard seafloors as shown in Fig. 8.21 in [2].
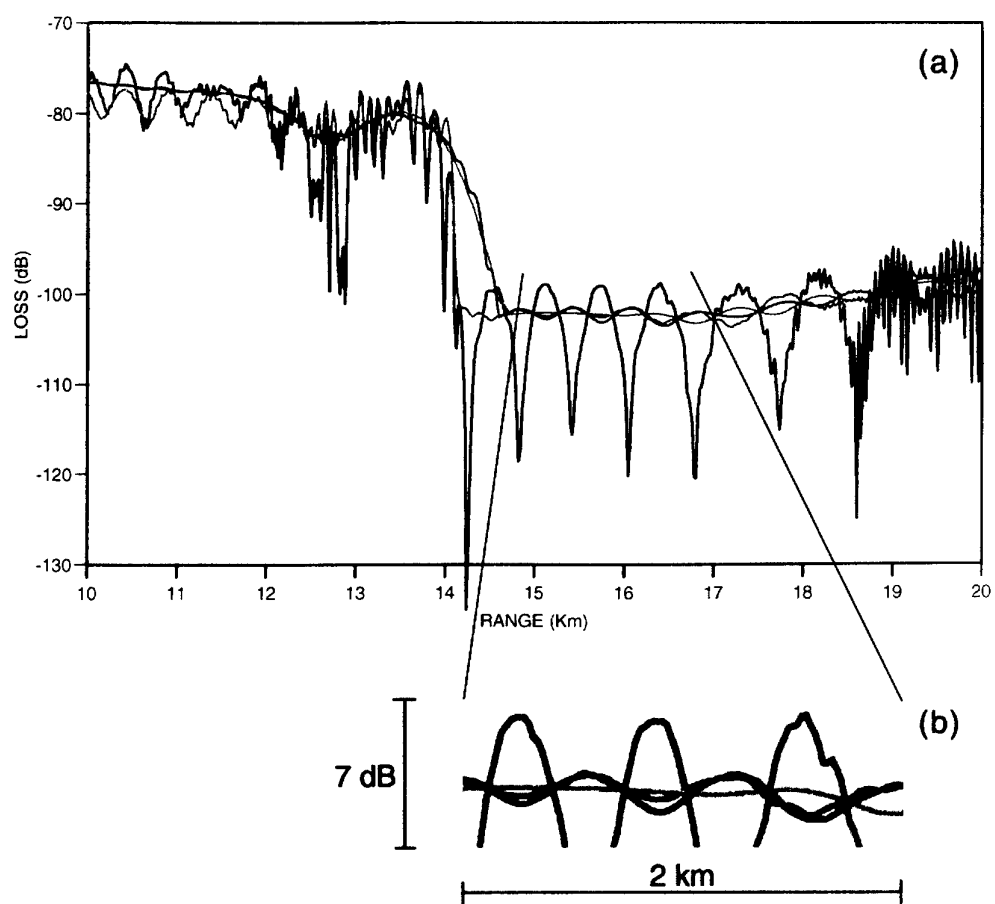
Figure 9 *(a) Propagation loss estimate (simulation) and average values. (b) zoom in reverberation zone.*
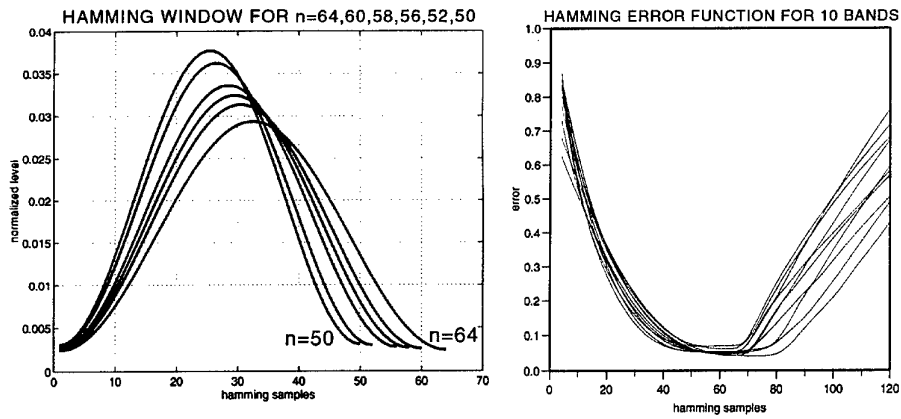
Figure 10 *Hamming windows utilized to calculate the average propagation loss and its error estimates compared to the conventional range and frequency averages.*
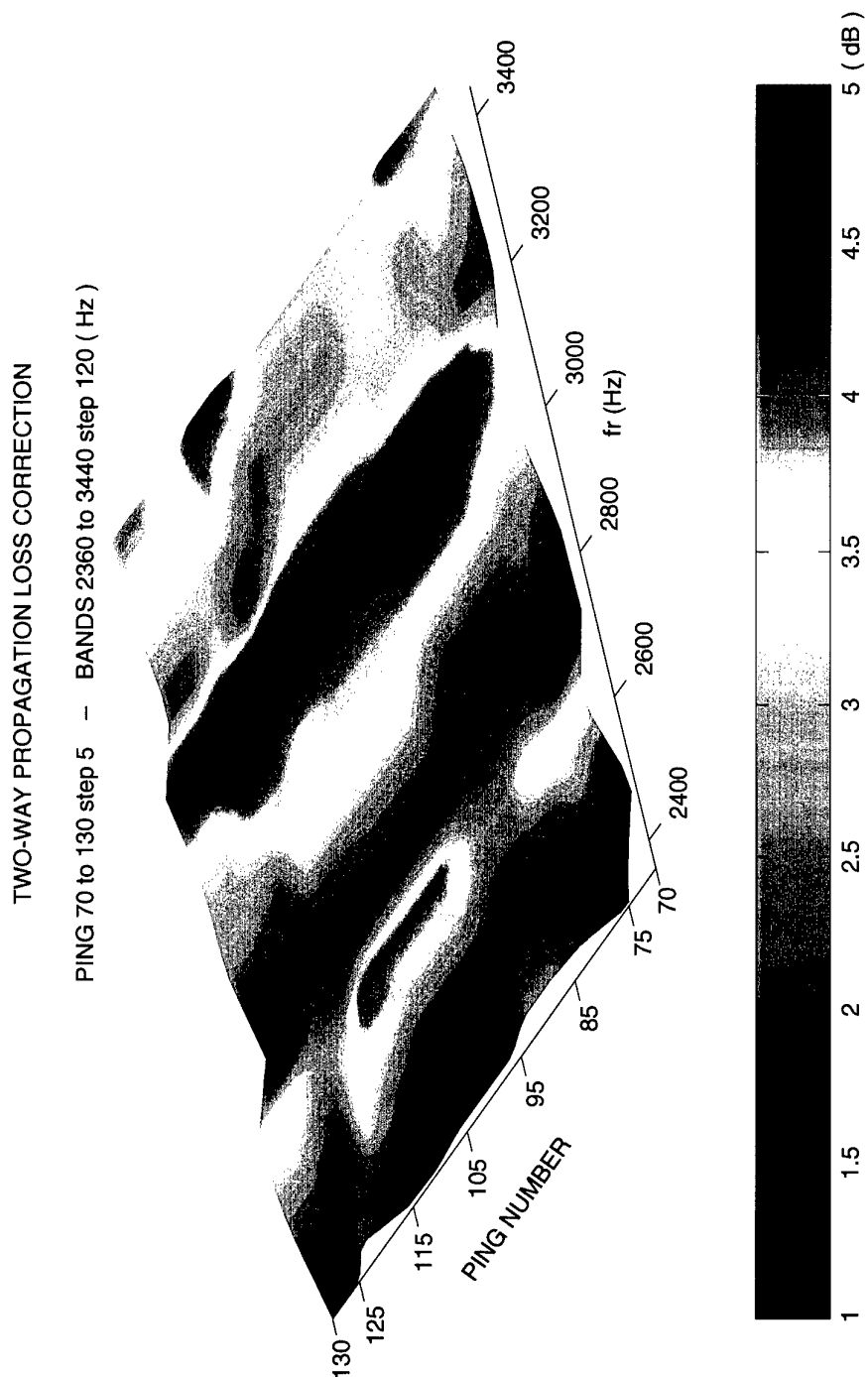
Figure 11   *Two-way propagation loss adjustment calculated according to the minimum propagation loss value of all pings and sub-bands.*
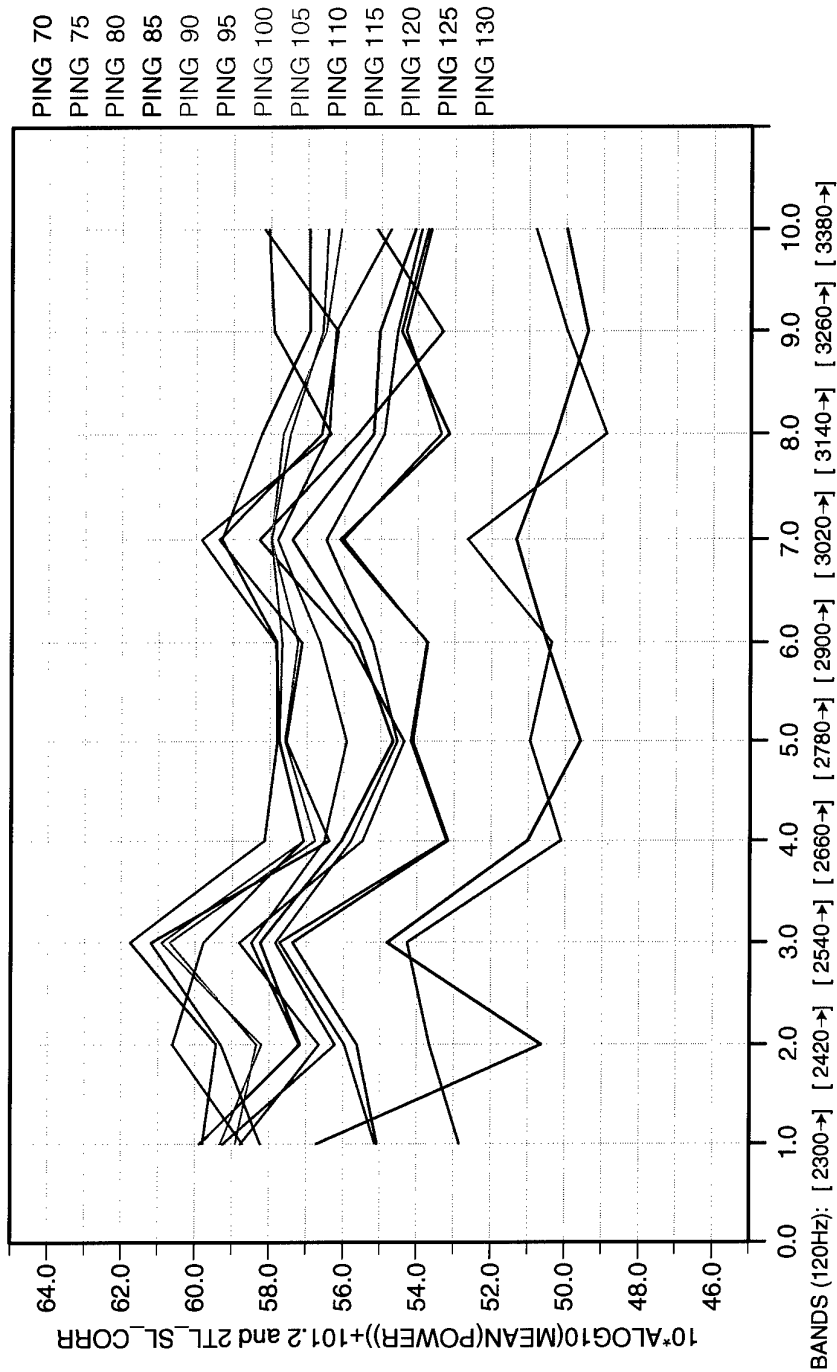
Figure 12 *Average reverberation power versus frequency (-sub-bands) after correcting for source spectrum and propagation loss.*

6

Conclusions

A sub-band processing scheme is devised to examine the frequency dependence of reverberation over a 1200 Hz linear frequency modulated signal. The transmitted spectrum is divided into ten equal sub-bands and an equal number of LFM replicas is independently correlated with the received signal. The MF correlator outputs are corrected according to the transmitted source spectrum and the two-way propagation loss.

Figure 13 demonstrates the three stages of this analysis: Part A corresponds to the raw MF output, part B to the source level correction, and part C the final adjustment based on two-way propagation loss. The comparison between A and B reveals that the original bias towards low frequencies is mainly due to the source power spectrum. The incorporation of the propagation loss introduced small variations in the ping (time) versus frequency surface without creating any prominent frequency trend. Independently of how accurate the model estimate is, one has to allow a few degrees of uncertainty, as the minor variations which are observed, lie within the statistical variation of the propagation loss estimates.

These results, compared with those produced for the active detection case described in [1], lead to the conclusion that the source utilized does not provide enough bandwidth to demonstrate significant target detection or reverberation variation as a function of frequency. It should be mentioned that the particular experiment was not designed for wide spectrum data analysis. For this reason and because broadband signal processing is an important area of research and development at SACLANTCEN, a new sea trial *Mercury 99* is executed having broadband analysis as one of its main goals.
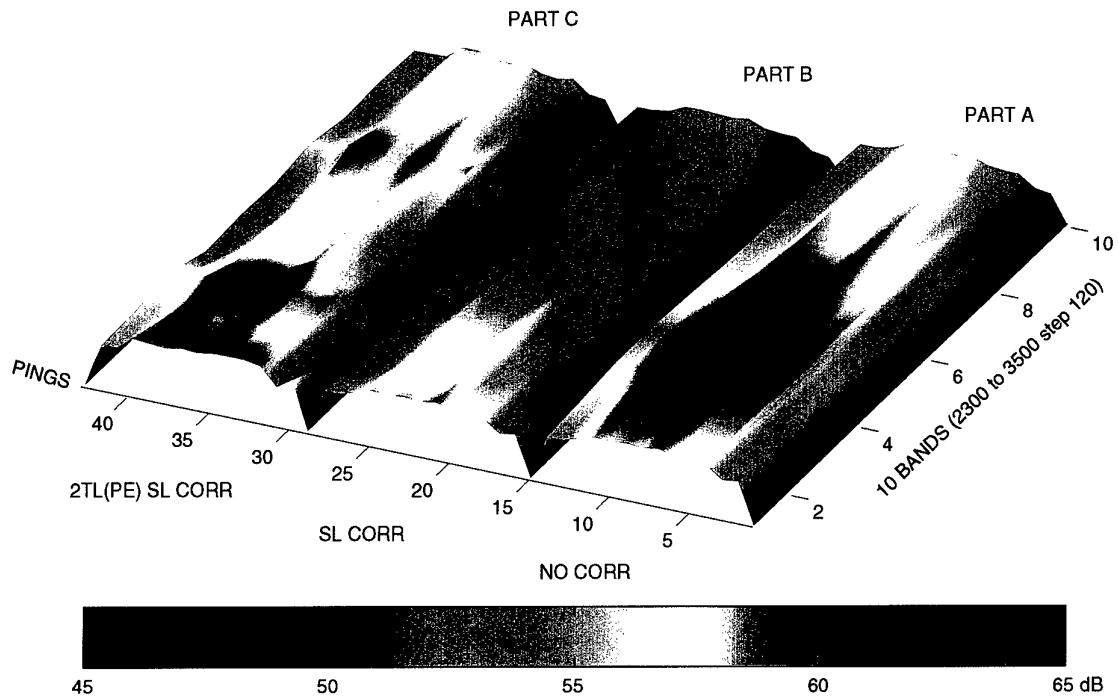
Figure 13 *Reverberation power versus frequency (sub-bands). Part A: calibrated data, part B: correction for source spectrum, part C: correction for source spectrum and two-way propagation loss.*

7
Acknowledgements

The authors would like to thank M. C. Ferla of the Modeling group at SACLANT-CEN for testing and selecting the appropriate computer model to simulated sound propagation for this particularly difficult range dependent scenario. Without his assistance the data analysis would have been incomplete.

References

[1] Haralabus G., Capriulo E., Zimmer W.M.X. SWAC 4: Broadband data analysis using sub-band processing, *SACLANTCEN* SR–320 2000.

[2] Urick, R.J. Principles of Underwater Sound for Engineers, *McGraw-Hill, Inc*, 1967.

[3] Dreini, G., Isoppo, C., Jensen, F.B. PC-based propagation and sonar prediction models, *SACLANTCEN* SR–240 1995.

[4] Ferla, M.C., Porter, M.B., Jensen, F.B. C-SNAP: coupled SACLANTCEN normal-mode propagation loss model, *SACLANTCEN* SM–274, 1993.

[5] Weinberg H., Keenan R.E. Gaussian ray bundles for modeling high-frequency propagation loss under shallow-water conditions. *Naval Undersea Warfare Centre, TR-10568* and *J. Acoustical Society of America* 100, 1421-1431, 1996.

<div style="text-align: right">

Annex A

Modeling

</div>

As the *in situ* propagation loss measurements were insufficient, the degradation of the sound energy due to the medium had to be predicted using acoustic models. A detailed analysis was performed to select the most reliable model suitable for the range-dependent environment of the experiment. Most of the following information is included in M. C. Ferla's conclusion report to the Head of the Signals and Systems Department.

The four models tested are: a) C-SNAP based on coupled mode technique, b) GRAB based on ray tracing, c) PAREQ based on parabolic equations, and d) RAM based on parabolic equations applying a split-step Pade' technique. OASES is used to obtain the bottom reflection values, which serve as input to the GRAB model. Each of these models is attractive for different reasons such as speed, accuracy, stability and user friendliness. For the challenging range-dependent environment, accuracy and stability are the principal objectives.
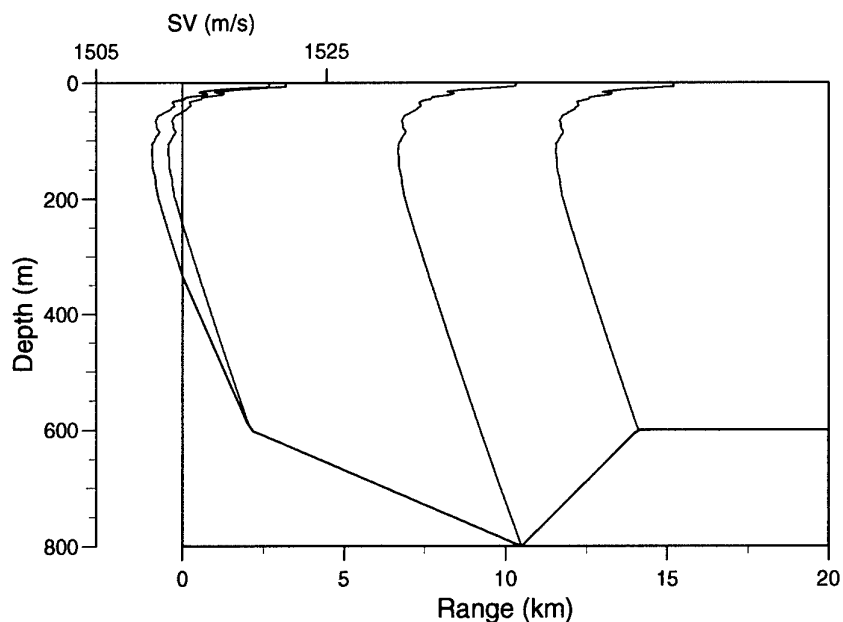

Figure A.1 *Plot of the seafloor bathymetry and sound velocity profiles in the water column.*

ENVIRONMENTAL PARAMETERS

The sound velocity profiles used in the water column are shown in Fig. A1. The first SVP is measured *in situ*. The rest are generated by extending the negative gradient segment to the appropriate depth. The sediment-water sound speed ratio is 0.98.

The values of the sound velocity in the sediment are:

sediment velocity

depth (m)	speed (m/s)
0.0	1482.25
10.0	1512.50
20.0	1527.62
30.0	1512.50
40.0	1527.62
50.0	1512.50

the water density 1.2 gr/cm^3 and the water column attenuation 0.5 dB per wavelength.

The geoacoustic parameters for the semi-infinite subbottom are the sediment density 2.0 gr/cm^3, the attenuation of compressional waves 0.5 dB per wavelength and the sound speed 1800 m/s.

The bottom reflection loss values obtained using the OASES model for 2900 Hz are shown in Fig. A2.

ANALYSIS

Range independent

The comparison of the four propagation models is managed in two stages. The first stage invokes two general assumptions: full beam aperture of ±32° and range independence. The former is necessary because at this maximum critical angle, the different beam types of all models are comparable. The latter serves as an intermediate step before modeling the range-dependent scenario. The geometrical parameters are shown in the next table

1st Test case parameters
water depth: 800 m
maximum range: 20 km
source depth: 68 m
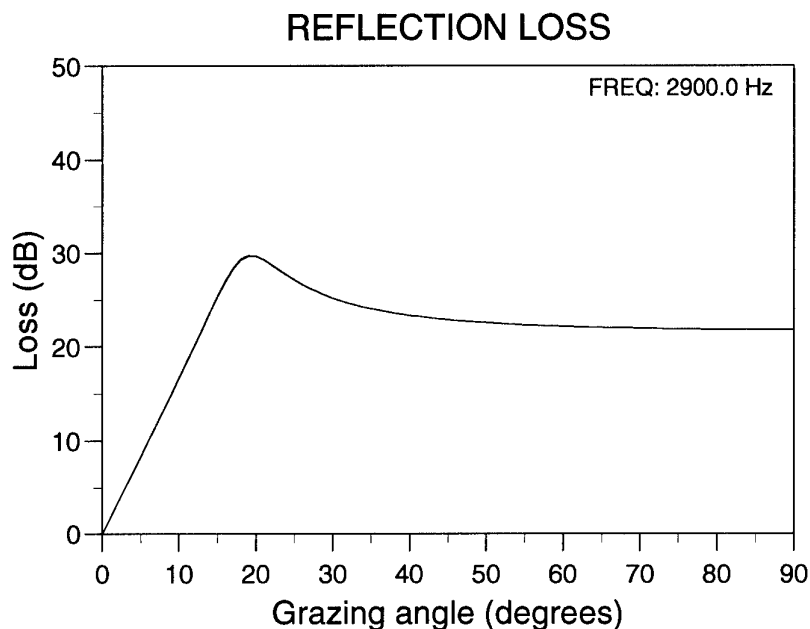receiver depth: 600 m
Frequency: 2900 Hz

REFLECTION LOSS

Figure A.2 *Sediment reflection loss versus grazing angle (model estimation based on OASES).*

Figure A3 shows the propagation loss estimates based on the following models:

Tested Models

Model	Color, type of line
GRAB	blue, solid
PAREQ	black, solid
RAM	red, solid
C-SNAP-1	green, solid
C-SNAP-2	green, dotted

With the exception of C-SNAP-1 (model run with the true attenuation values), all the models are in agreement regarding the average propagation loss values. The reason C-SNAP-1 demonstrates severe energy loss in the first 6 km resides in its natural limits to accurately compute attenuation sediment for higher order modes. As a result, the downward refracted rays which bounce off the seafloor at the first 6 km undergo an unrealistically large energy loss. This is confirmed by the C-SNAP-2 case in which the same model is used with an arbitrarily low attenuation factor for the sediment. The high-angle rays are of extreme importance in this range-dependent case, because after bouncing off the seafloor and the sea surface they remain the main energy carriers at the reverberation area between 14.5 and 15.5 range, as seen in Fig . A4 (contour plot of the PAREQ model). C-SNAP propagation

– 25 –

loss estimate diverges from the mainstream predictions of the other models because of its poor treatment of the attenuation associated with steep propagation angles. For this reason the C-SNAP is excluded from the case test.

Range dependent

The outcome of the range dependent case is shown in Fig. A5. The agreement between PAREQ (solid black line) and RAM (solid blue line) is perfect. GRAB is used with two different input parameters set. The dotted red line represents a case which does not consider the sediment phase values. The solid red line is the GRAB case which includes the phase information. The incorporation of phase information in the GRAB model improves the propagation loss prediction for ranges greater than 15 km, although for ranges less than 15 km, GRAB predictions differ significantly from those of PAREG and RAM.

Conclusion - PAREQ

In conclusion, the PAREQ and the RAM models proved to be more stable and suitable than GRAB and C-SNAP for the particular simulation. From these best performance models, PAREQ is preferred to RAM because it possesses two additional advantages: a) it is more user-friendly and b) has the ability to model Gaussian beams for the transmitted energy.
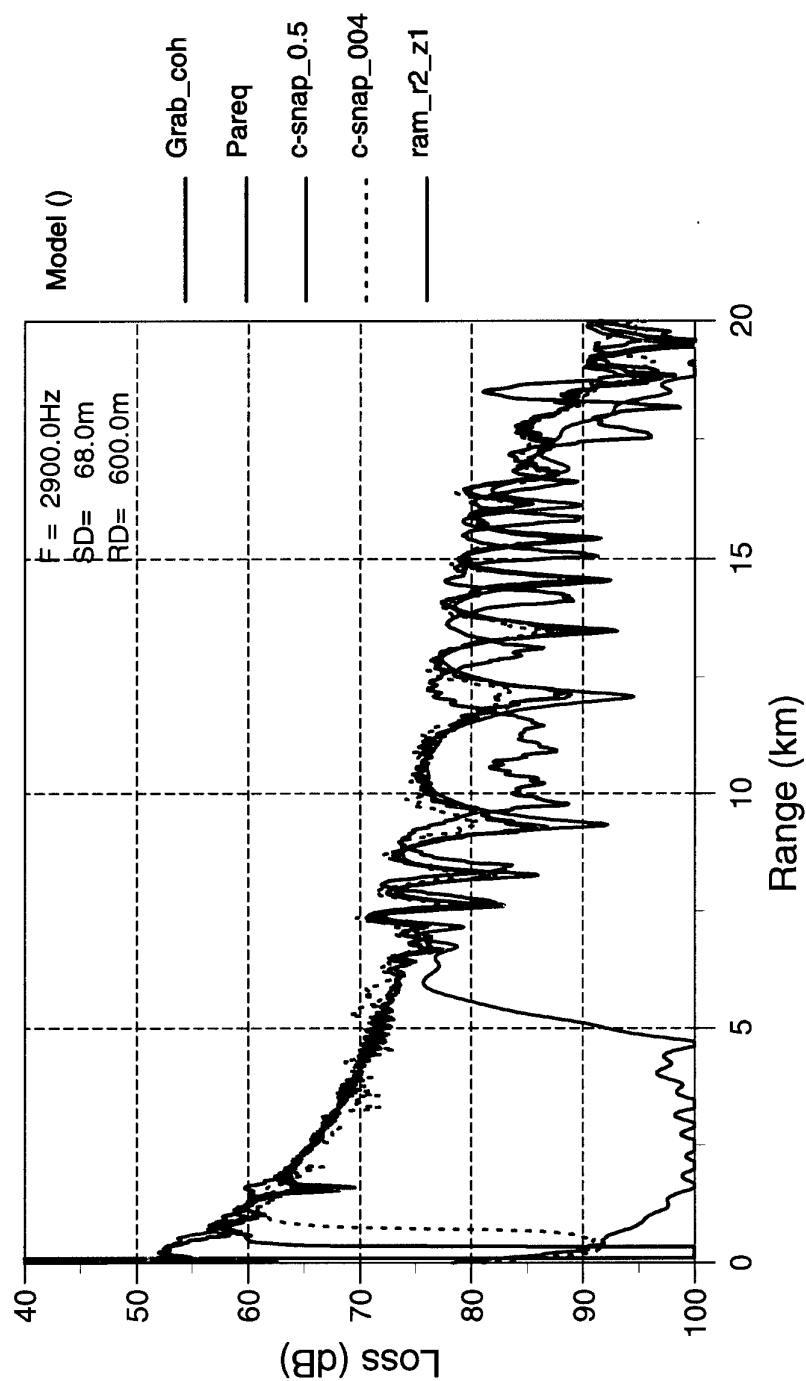
Figure A.3 *Range independent case model comparison: C-SNAP with actual bottom attenuation (green solid), C-SNAP with arbitrarily small bottom attenuation (green dotted), PAREQ (black, solid), RAM (red, solid), GRAB (blue, solid) comparison.*
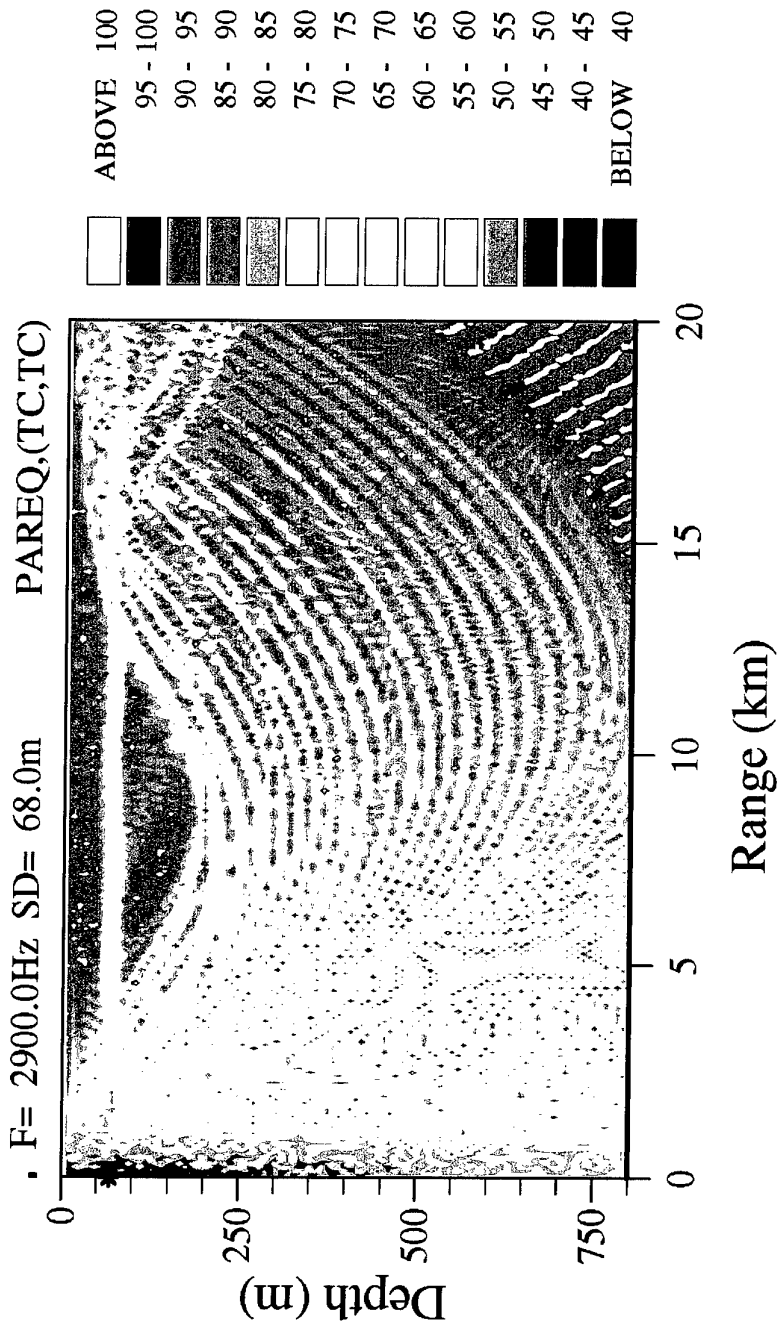
Figure A.4 *PAREQ contour propagation loss plot to demonstrate steep angle energy arriving at 15-20 km after bouncing of the seafloor and the surface.*
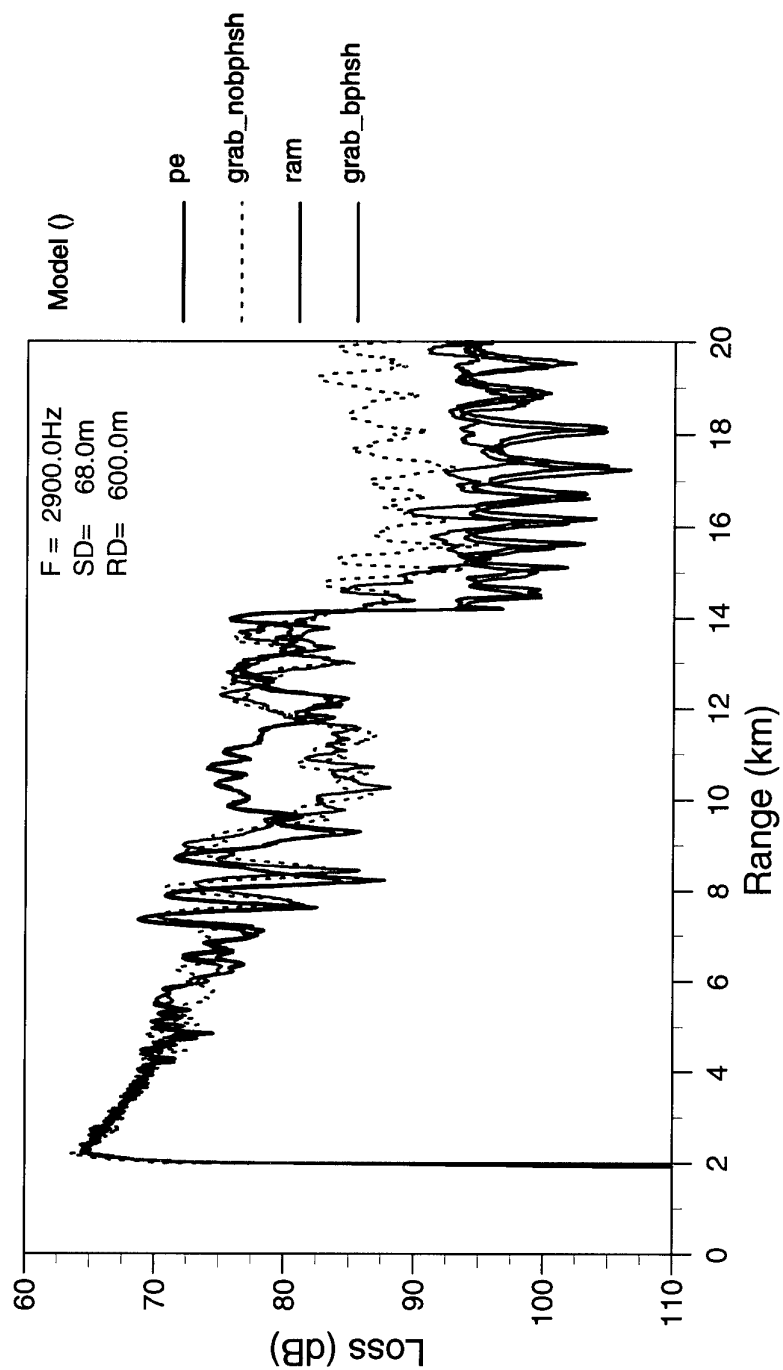
Figure A.5 *Range dependent case - Model comparison: PAREQ (black, solid), RAM (blue, solid), GRAB with sediment phase (red, solid) GRAB without sediment phase (red, dotted) comparison.*

Document Data Sheet

Security Classification	Project No.
UNCLASSIFIED	04-A

Document Serial No.	Date of Issue	Total Pages
SR-337	December 2000	35 pp.

Author(s)

Haralabus, G., Capriulo, E.

Title

SWAC 4: Broadband data analysis using sub-band processing – part II.

Abstract

The frequency dependence of reverberation is examined using the processing method as for the frequency analysis of target detection during the same experiment.

In this experiment, reverberation is induced by abrupt changes in the bottom bathymetry (a 200 m sea mount). For the analysis of the received signal a sub-band matched filter scheme is devised, according to which, a replica of the transmitted pulse (2300 Hz-3500 Hz LFM signal) is segmented into ten 120 Hz sub-bands, each of which is processed independently through a matched filter detector. Following the necessary corrections for array gain and calibration, transmitted power spectrum and propagation loss, the matched filter data are compared to reveal the frequency dependence of reverberation. Due to insufficient *in situ* measurements, the propagation loss estimate is based on model calculations – a challenging task for the range dependent seafloor at the experimental site.

After examining a large number of pings it is concluded that the reverberation energy calculated at the correlator output is comparable for all ten sub-bands. This leads to the conclusion that for the particular environment and experimental geometry, the frequency spectrum is not sufficiently wide to allow significant frequency variability which may indicate an optimum operational frequency.

Keywords

Reverberation – broadband analysis – sub-band processing – frequency variability